Chapter 4

Magnetic-ordering of polycrystalline Yttrium Iron Garnet thin film

Abstract

YIG is a ferrimagnetic insulator with significant potential in various applications, such as magnonics, microwave oscillators, and optical devices [18, 133]. This chapter highlights that the sol-gel-based spin coating method can be utilized as an effective way to deposit excellent quality YIG thin films. Consequently, the present chapter deals with optimizing the growth process of YIG thin film using an all solution methods. Here, we report the growth of uniform polycrystalline YIG thin films on thermally oxidized Si (100) substrates with variable annealing durations. The sample's phase confirmation and elemental analysis with an ionic environment were conducted using the XRD and the XPS, respectively. The magnetic studies in the present work using FMR depicts that the YIG sample annealed for 5 hrs shows the lowest Gilbert damping constant α = 4.7 $\pm$ 0.4 $\times$ 10^{-3} with an

inhomogeneous damping contribution to the linewidth of 5.0 ± 0.3 mT which is lowest among the previous studies of using the all solution methods [45, 134].

4.1 Introduction

YIG crystal has a cubic crystal structure with space group $Ia\bar{3}d$ [135, 136]. Magnetic ion Fe^{3+} in the unit cell of the crystal structure form a tetrahedron and octahedron with oxygen ions; these coordinations are antiferromagnetically coupled, as they are not equal in numbers and give rise to ferrimagnetic ordering [135, 137]. Understanding the magnetization dynamics of YIG is a fascinating research topic due to its various applications, mainly in microwave absorbance [138], acoustic transducers [139], and magneto-optical devices [140, 141]. Studying YIG is also essential due to its manifestation of spin Seebeck effect in Bismuth-doped YIG [142]. Recently, YIG's application in spin-pumping has emerged and initiated various studies [143, 144, 17]. Investigating the magnetic energy dissipation factor of the YIG materials with lower α is desirable for the larger magnon propagation length and its application in magnonics [145]. In the past YIG has been grown using sophisticated deposition methods like liquid phase epitaxy, PLD, and sputtering [144, 146, 147, 148, 90, 149, 150, 93, 151]. The observed value of α for YIG varies between 5.16×10^{-5} to 1.2×10^{-1}[144, 146, 147, 148, 90, 149, 150, 93, 152, 153, 151, 91, 154, 155, 81]. The reported values of α for polycrystalline YIG deposited using co-precipitation spin-coating are ranging 2.7×10^{-2} to 1.2×10^{-1}[134]. The lower the α, the higher the possibility YIG can be utilized for practical applications.

This chapter presents a cost-effective all-solution process-based spin-coating method to deposit the YIG thin film on thermally oxidized Si substrates. We prepared the thin films, studied them with varying annealing durations, and optimized the appropriate annealing duration. After the optimization of the annealing duration, we determine the intrinsic and

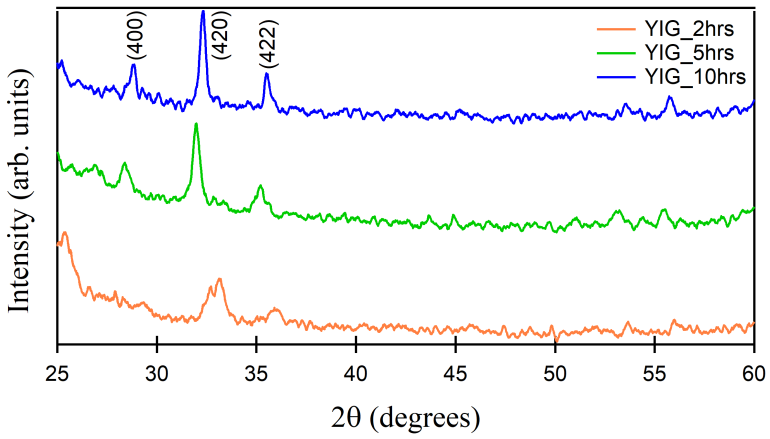

Fig. 4.1 *X-ray diffraction of YIG annealed at 2 hrs, 5 hrs, and 10 hrs.*

extrinsic magnetic energy dissipation factors of grown YIG films using FMR techniques. We observe the lowest damping constant of sol-gel-based spin-coated YIG films compared to previous studies [45, 156].

4.2 Results and Discussion

4.2.1 Structural Study

Figure (4.1) shows the XRD pattern of the deposited YIG thin films; major peaks (400), (420), and (422) have been indexed using JCPDS no. 00-033-0693 [45, 157, 158]. The lattice parameters a=b=c for YIG thin films annealed at 2hrs, 5hrs, and 10 hrs are 1.2129 nm, 1.2509 nm, and 1.2384 nm, respectively, with $\alpha = \beta = \gamma = 90$ °C. The highest intensity peak (420) was fitted using the Lorentz fitting, and the full width at half maxima was used to calculate Scherrer's crystallite size [159]. The crystallite sizes calculated are 9 nm ± 1, 20 ± 1 nm, and 28 ± 1 nm of YIG annealed at 2 hrs, 5 hrs, and 10 hrs, respectively. These details are provided in table (4.1).

With increasing annealing duration, XRD peaks get more intense and sharpened due to increasing grain size with the increase in annealing duration, which is well corroborated

Table 4.1 *Lattice parameters and grain size of the deposited polycrystalline YIG.*

Sample	lattice parameters		Crystallite size (nm)
	a=b=c (nm)	$\alpha = \beta = \gamma$(deg)	
YIG 2 hrs	1.2129	90	9
YIG 5 hrs	1.2509	90	20
YIG 10 hrs	1.2384	90	28

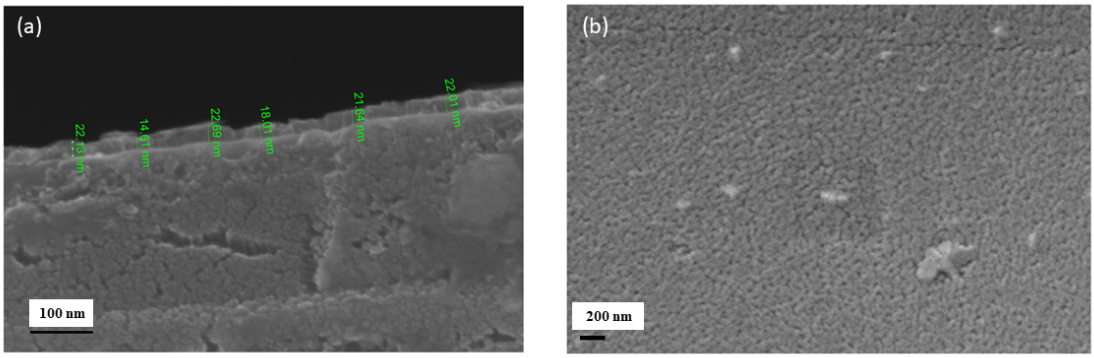

Fig. 4.2 *Scanning electron microscopy image of YIG thin film annealed for 5 hrs (a) cross-section image for thickness estimation and (b) surface morphology of homogeneous polycrystalline YIG film.*

by literature [160]. To get single-phase YIG with good crystallinity, annealing of 5 hrs or more is required, as confirmed by XRD.

4.2.2 Thickness Analysis and Surface Morphology

Figure (4.2)(a) displays the cross-sectional SEM of sol-gel-based deposited YIG. The marked green area is YIG thin film, and the average deposited thickness of the film is 20 ± 3 nm. Figure (4.2)(b) displays the SEM image of spin-coated YIG. It confirms the polycrystalline deposition that shows the growth is uniform over the substrate. The grains have covered the substrate homogeneously. Few larger grains are also observed, but uniform coverage of nm-sized grains on the substrate dominates. The absence of cracks in thin films was prominent in a few of the previous studies of YIG using the sol-gel-based spin-coating [161, 162].

4.2.3 Elemental and Ionic Environment Study

Figure (4.3)(a) depicts the wide-range survey scan XPS spectra recorded for synthesized YIG films. Characteristic photoemission and Auger peaks of Y, O, C, N, and Fe (YIG film) confirm the chemical pureness of the grown YIG films. The composition of Y and O are not much varied in the samples studied [163, 164]. Survey scans of all three annealed samples show the same binding energy position, with some intensity variation. Figure (4.3)(b) depicts the high-resolution spectra of the O_{1s} orbital. Inset of Figure (4.3)(b) shows the ratio of the surface and the bulk oxygen ratio. The ratio between the area of 531.3 eV and 529.6 eV peaks has been presented. The variation between 2 hrs and 5 hrs ratio is low, 0.4, and is within the error bar of the area estimation of the software. The 10 hrs sample has a lower area ratio than the 2 hrs and 5 hrs samples. This concludes the presence of oxygen vacancies in the 10 hrs sample. This can be further confirmed with lattice parameter reduction in the XRD as an annealing duration is increased after 5 hrs when the initial crystalline phase has formed. Furthermore, as the oxygen vacancy forms, Fe and Y remain confined in a similar crystal structure, but the absence of oxygen in the unit cell causes the lattice distortion, resulting in the shrunken lattice parameter as observed in YIG 10 hrs (a = 1.238 nm) comparatively to the YIG 5 hrs (a = 1.251 nm) shown in Table 4.1 [165].

After analyzing the XRD and the XPS, we concluded that YIG 2 hrs did not have complete phase formation and that YIG 10 hrs had oxygen vacancy. Subsequently, the YIG 5 hrs sample was analyzed for the high-resolution XPS study. The Y (3d), O (1s), and Fe (2p) XPS spectra are shown in higher resolution in Figure (4.4)(a-c). Figure (4.4(a) presenting the deconvoluted O_{1s} XPS spectra after linear background subtraction. Two peaks at binding energies 529.6 eV and 531.3 eV are due to the presence of O_{1s} in the thin film along with the surface oxygen [163]. The peak on the high binding energy side is supposed to be related to the hydroxyl group due to YIG surface exposure. As shown in Figure (4.4

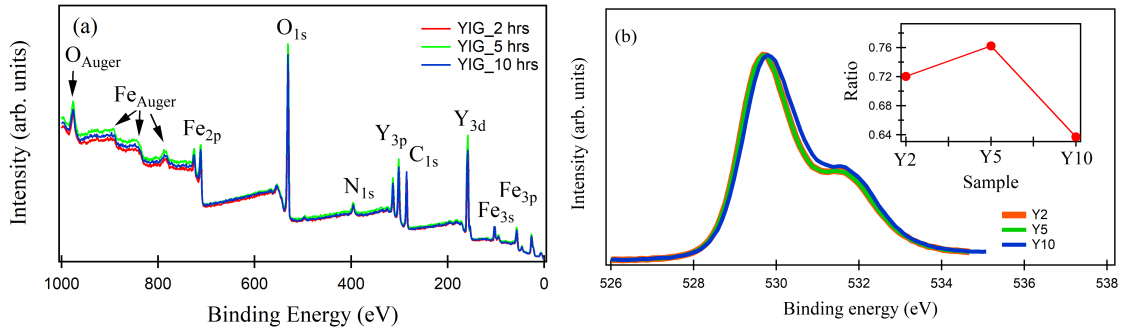

Fig. 4.3 *(a) XPS survey scan of the varying annealing duration of sol-gel-based spin-coated YIG thin films. (b) The high-resolution O_{1s} XPS spectra of YIG 2 hrs, 5 hrs, and 10 hrs, and the inset shows the area ratio of the 531.3 eV and 529.6 eV peaks of the YIG 2 hrs, 5 hrs, and 10 hrs.*

(b), the prominent peaks for Y (3d) are at binding energy 159.5 and 157.4 eV for $Y_{3d_{3/2}}$ and $Y_{3d_{5/2}}$, respectively that matches with the literature [166].

The Fe $2p_{3/2}$ and $2p_{1/2}$ peaks are positioned at 710.3 and 723.9 eV, respectively, as shown in Figure (4.4)(d). The positions of Fe 2p peaks are used to estimate the presence of $Fe^{2+/3+}$ valence at their ratio. Due to the existing uncertainty of absolute positions of Fe^{2+} and Fe^{3+} peaks, it is feasible to identify Fe^{3+} from $Fe^{2+/3+}$ by the satellite peaks that show up across the higher binding energy side of the $2p_{3/2}$ peak at a distance of $\sim$ 8 eV for pure Fe^{3+} and $\sim$ 6 eV for pure Fe^{2+}. In XPS studies, the Fe^{3+} satellite peak is observed, indicating the dominating nature of Fe^{3+} valence state. Thus, it is likely that the Fe^{3+} state characteristic for bulk YIG is mostly obtained in thick YIG film, while in the ultra-thin YIG film. As the Fe^{3+} is present in two different environments, i.e., tetrahedral Fe_{tetra} and octahedral Fe_{oct} coordinates. For $Fe_{2p_{3/2}}$, the theoretical intensity ratio of Fe_{oct} and Fe_{tetra} is 2:3 and the experimental calculations gives it to 0.61. For $Fe_{2p_{1/2}}$, the theoretical area ratio is similar, and the experimental calculations give it to 0.65. The average of two gives the ratio of 0.63, close to the theoretical ratio of 0.66. The assumption of linear background in analysis causes the error. Figure (4.4)(d) presents the deconvoluted Fe_{2p}

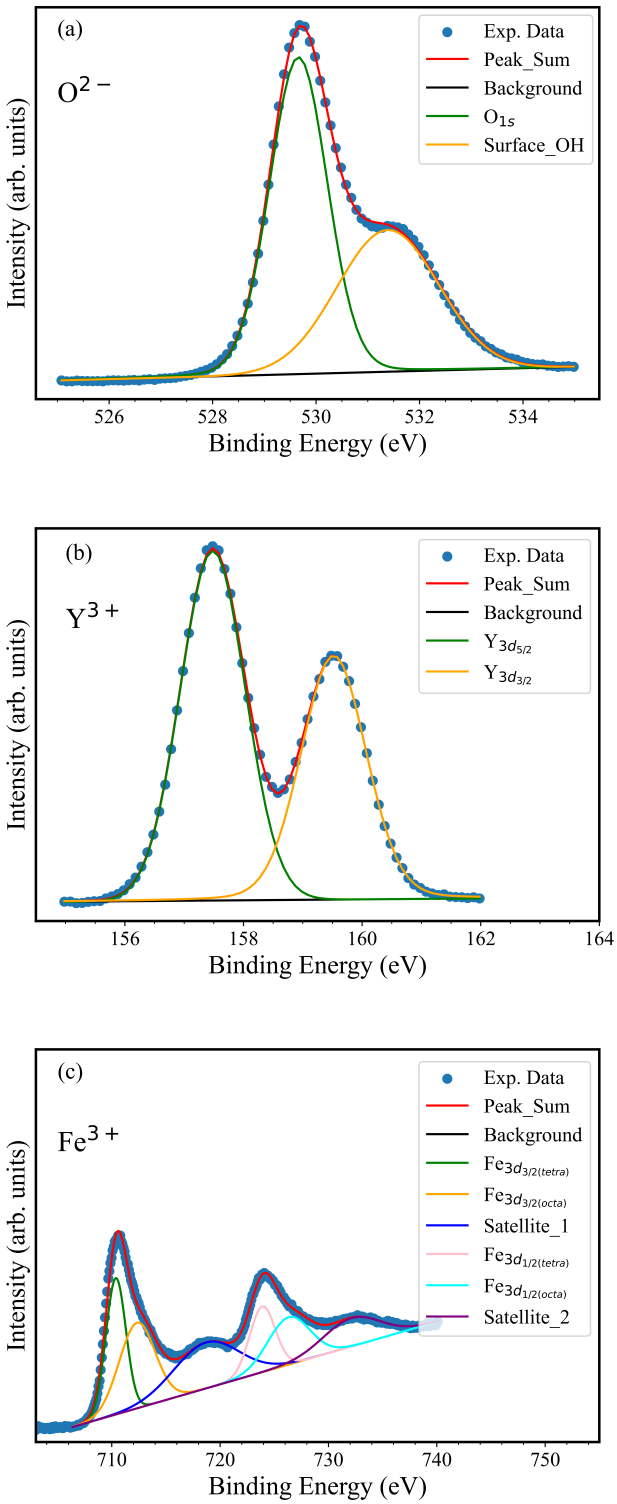

Fig. 4.4 *(a) High resolution deconvoluted XPS spectra of (a) O_{1s}, (b) Y_{3d}, and (c) Fe_{2p} energy levels.*

XPS spectra after linear background reduction. There are prominent peaks at 710.3 eV and 723.9 eV of Fe $2p_{3/2}$ and Fe $2p_{1/2}$ energy levels, respectively [167, 168]. Table 4.2 shows the experimentally obtained atomic percentage of Y, Fe, and O in the deposited sample. The atomic percentage is calculated using CasaXPS software [169]. The atomic percentage of Oxygen is 60%, Iron is 22%, and Yttrium is 18%. The experimental atomic percentage agrees with the expected atomic percentage of the YIG [166].

Table 4.2 *Atomic percentage of elements in polycrystalline YIG obtained in this study.*

Element	atomic %	Valence state
Oxygen	60	2-
Iron	22	3+
Yttrium	18	3+

4.2.4 Magnetic Study

The magnetic study of the YIG is performed using the SQUID-VSM magnetometry. Figure (4.5) depicts the magnetization as a function of the magnetic field of YIG 2 hrs (red), YIG 5 hrs (green), and YIG 10 hrs (blue) at 300K in in-plane orientation. Magnetization in emu/cc is converted to the μ_B/f.u. using the equation given below [170]:

$$\mu_{B_{exp}}/f.u. = \frac{M * M_w}{\rho * N_A * \mu_B} \tag{4.1}$$

where, M is magnetization (emu/cc), M_w is molecular weight (737.93), ρ is the density of YIG (5.019 g/cm^3), N_A is Avogadro number (6.022×10^{23} mol^{-1}), and μ_B Bohr magneton (9.274×10^{-24} J/T). The coercivity of the three samples has been studied, were estimated to be 0.4 $\pm$ 0.2 mT, 0.1 $\pm$ 0.1 mT, and 1.4 $\pm$ 0.3 mT for the YIG 2 hrs, 5 hrs, and 10 hrs. The saturation magnetization of all three samples varies non-monotonic. YIG 5 hrs have the highest saturation magnetization at 3.13 $\pm$ 0.03 μ_B/f.u. which is similar to the nanoparticles synthesized using the nitrates-based sol-gel method [171, 172], and

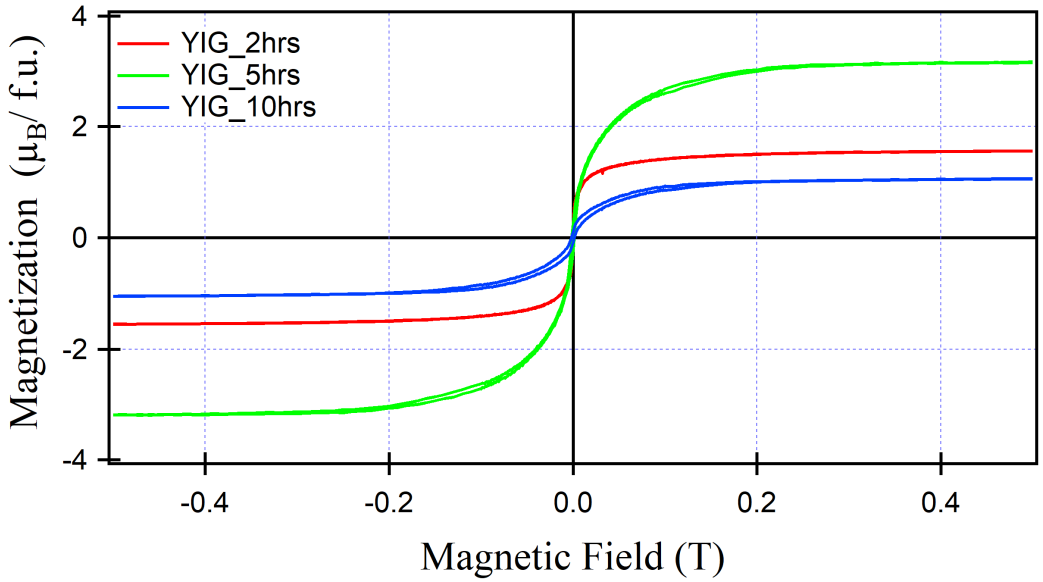

Fig. 4.5 *M-H loops of YIG 2 hrs, YIG 5 hrs, and YIG 10 hrs measured at room temperature.*

the rf-sputtering deposited YIG thin film [140]. As the XPS confirms, stoichiometry is maintained, and the phase analysis gives higher quality nanoparticles formed by the nitrates precursor with the optimized annealing temperature and duration, resulting in the excellent quality polycrystalline deposition of the YIG at 5 hrs, consequently in the higher saturation magnetization and lower coercivity [173]. The nanoparticles of the three samples form a uniform film over the substrate and behave as a multi-domain structure, and the high crystallinity reduces the pinning sites, which reduces the steps to switch the magnetization and, subsequently, the lower coercivity in the present work. The step size taken for the applied field was 1 mT, and the variation of the coercivity is similar to it for all three samples, showing they have a similar order of the coercivity. The saturation magnetization of the YIG 2 hrs is lower because of the poor phase formation, and the YIG 10 hrs has the lowest saturation magnetization; as the XPS suggests, it has the oxygen vacancy to suppress the super-exchange interactions. The magnetic moment reduces with the suppression of the exchange interaction, resulting in a reduction of saturation magnetization [174]. The

decrease in the magnetization is because of the oxygen vacancy in YIG 10 hrs. YIG 5 hrs sample's high saturation magnetization makes it most suitable for further studies.

4.2.5 Ferromagnetic Resonance Study

Figure (4.6) depicts the change in the derivative of absorbance as a function of the applied field for the YIG 2 hrs, YIG 5 hrs, and YIG 10 hrs in orange, green, and blue color samples, respectively. The YIG 2 hrs sample shows direct absorption at 0.2139 T. The YIG 5 hrs sample shows a sharp resonance peak at 0.2208 T, confirming single-phase YIG. As the deposited thin films have been heated for a longer time, e.g., 10 hrs, causing the oxygen vacancies as confirmed using the XRD, XPS, and magnetometry. The suppressed magnetic interaction results in a low absorption FMR signal at 0.2778 T. The optimum annealing duration for YIG synthesis using all sol-gel-based spin coating was 5 hrs at 900 °C. The

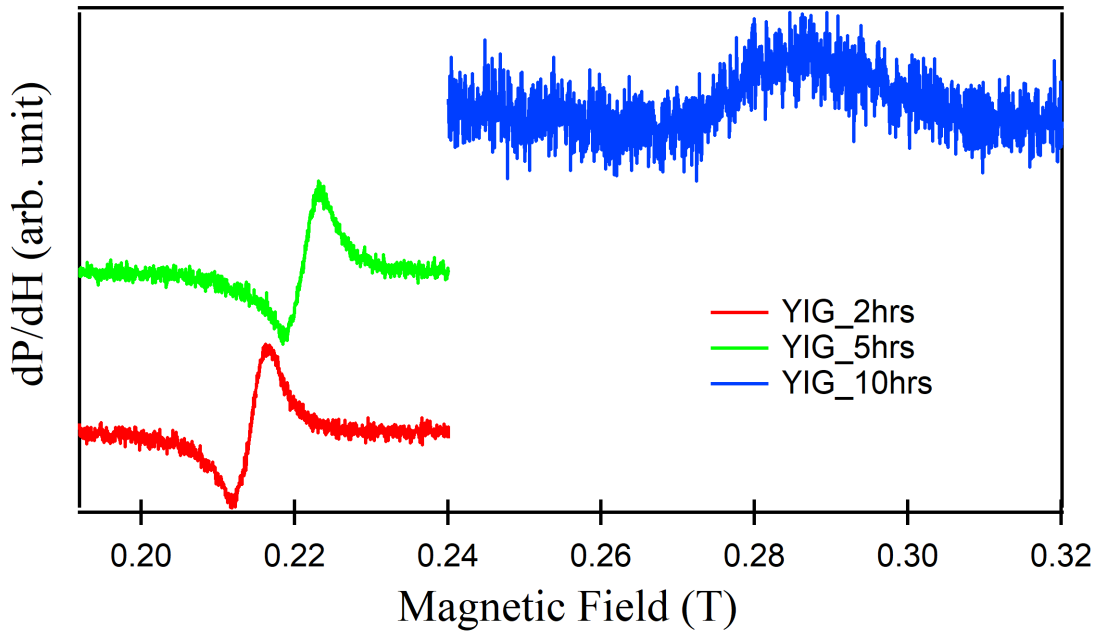

Fig. 4.6 Derivative of phase as a function of applied DC magnetic field of YIG 2 hrs, YIG 5 hrs, and YIG 10 hrs.

magnetic dissipation factors, the damping constant, and the inhomogeneous contribution of granular deposited YIG 5 hrs are studied and discussed further.

Figure (4.7)(a) shows the FMR spectra in the in-plane geometry of the sol-gel-based spin-coated YIG film. The first derivative of the absorbance of the microwaves at all frequency from 3.5-15.5 GHz at the step size of 1.5 GHz as a function of the applied dc magnetic field is highlighted. The derivative of the Lorentzian equation is used to fit the data. The linewidth of the resonance is a result of dissipative elements in the dynamics of the materials [175]. Figure (4.7(b) is resonant frequency as a function of resonance magnetic field (H_{res}). Experimental data were fitted using the Kittel equation [164] given below:

$$f = \left(\frac{\gamma}{2\pi}\right)\sqrt{(\mu_0 M_{eff} + H)(H)} \tag{4.2}$$

where γ is the gyromagnetic ratio, μ_0 is permeability, and M_{eff} is effective magnetization. Fitted data calculates the value of $\mu_0\, M_{eff}$ = 0.1887 $\pm$ 4.5$\times 10^{-3}$ T and $\gamma/2\pi$ = 26.64 $\pm$ 0.11 GHz/T. The value of the experimental g-factor is 1.919. g-factor is calculated using a simple equation g= $\frac{\gamma\hbar}{mu_B}$ As the sample is grown using sol-gel-based spin coating, the thin film's grains are assembled randomly assembled. Due to the randomization of these grains, net anisotropy was absent in the sample. Dissipation of energy is important in knowing the spin-wave damping behavior of the thin film [145].

The sample's damping constant (α) is analyzed by linear fitting the linewidth as a function of frequency as shown in Figure (4.7)(c). As at lower frequencies signal to noise ratio is low, over or under-estimation of linewidth occurred. Therefore, experimental linewidth data has a slight deviation from fitted data. Linewidth as a function of frequency has been fitted using an equation showing the relation of frequency, and the damping parameter is as follows[146, 147, 176]:

$$\Delta H = \Delta H_0 + \left(\frac{4\pi\alpha}{\gamma}\right) f \tag{4.3}$$

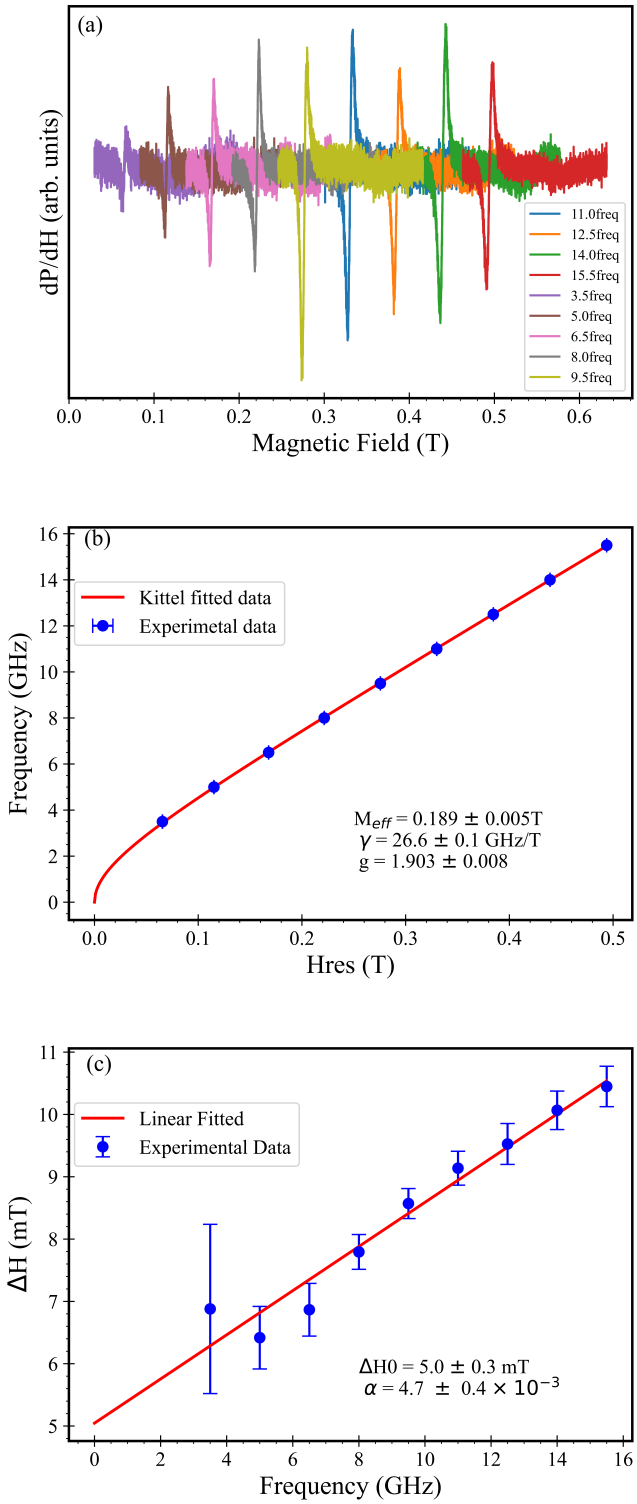

Fig. 4.7 *The room temperature FMR study of the YIG 5 hrs sample (a) derivative of phase of variable frequencies 3.5 - 15.5 GHz at the step size of 1.5 GHz as a function of applied DC magnetic field, (b) frequency is plotted as a function of resonance magnetic field and fitted using Kittel formula, and (c) experimental linewidth (ΔH) has been plotted as a function of frequency and fitted linearly.*

where ΔH is linewidth, ΔH_0 is an extrinsic contribution to the linewidth, α is Gilbert damping constant, a result of intrinsic dissipation, and f is applied frequency. Equation (4.3) is utilized to fit the plot of linewidth as a function of applied frequency. This linear fit gives $\alpha = 4.7 \pm 0.4 \times 10^{-3}$ and $\Delta H_0 = 5.0 \pm 0.3$ mT. Sol-gel-based deposited YIG/Si shows higher damping parameter than the PLD and ion beam sputtering deposited films on GGG substrates [152, 154, 177]. M_{eff} value is higher in this work comparing the previous works and than the SQUID-VSM magnetization value. The reason was not resolved with the present experiments; further anisotropy study can resolve these factors. Here, the value of ΔH_0 suggests that the major contribution in linewidth is inhomogeneity of film [178], which is comparably higher than the previous work on the YIG/GGG interfaces of the value less than a mT [149, 90, 93]. Table 4.3 depicts the comparative study of the present work and the available literature. It gives how the substrate and method of deposition affect the $\mu_0 M_{eff}$ and Gilbert damping parameter values [134]. YIG deposited on the Gadolinium Gallium Garnet (GGG) substrate has the lowest damping parameter as observed in Table 4.3, as the lattice mismatch between YIG and GGG is the lowest and it is the epitaxial thin film and resultant has higher crystallinity and fewer defects, making it an excellent magnon propagation conduit. Earlier spin-coating-based literature on the YIG deposition presented a high value for the damping parameter [134]. In this work, the α value is reduced because of the excellent crystallinity of the sample due to the optimized annealing temperature and duration to get a homogeneous crack-free surface. The XRD, XPS, and SEM present the qualitative and quantitative analysis of the deposited thin films, which importantly support the present FMR result. In spin-coating, the grain boundaries present in YIG significantly contribute to the inhomogeneous dissipation of the magnetic energy. The presence of 5.0 ± 0.3 mT inhomogeneous contribution shows that the individual grains are causing this dissipation in extrinsic mode. This suggests that the polycrystallinity of the sol-gel-based deposited YIG significantly contributes to

the magnetic energy dissipation, as the quartz substrate film also shows by PLD growth [179]. The intrinsic dissipation of sol-gel-based deposition presented in the present article is better than the PLD-deposited YIG on Quartz. Magnetic dissipation in the sol-gel-based spin coating on Si substrate is higher than the PLD or liquid phase epitaxy deposited YIG on GGG substrates, but when considering the cost-effectiveness, the sol-gel-based spin coating needs to be studied elaborately as done in the present study.

Table 4.3 Comparing the effective magnetization ($\mu_o M_{eff}$) and Gilbert damping parameter literature with the present sol-gel prepared polycrystalline YIG 5 hrs.

Substrate	Deposition Method	$\mu_o M_{eff}$ (T)	Damping Parameter	reference
SiO_2/Si	Sol-gel-based spin-coating	0.1887	4.7×10^{-3}	Present
Quartz	PLD	0.1620	1.6×10^{-2}	[179]
Si	Co-precipitation spin-coating	0.1734	2.7×10^{-2} to 1.2×10^{-1}	[134]
SiO_2/Si	PLD	0.1633	1.9×10^{-3}	[152]
GGG	Sputtering	0.1770	1.03×10^{-3}	[93]
GGG	PLD	0.1300	3.5×10^{-4}	[90]
GGG	PLD	0.1700	2.3×10^{-4}	[149]

4.3 Summary

Using sol-gel-based spin-coating on thermally oxidized Si(100) substrate, YIG is successfully deposited and the structure is modified with varying annealing durations of 2 hrs, 5 hrs, and 10 hrs. At 5 hrs, highly crystalline phase formation was confirmed with the XRD with a relaxed lattice parameter. The XPS study shows the oxygen-vacancy in the 10 hrs sample that significantly reduced the saturation magnetization and the absorption of microwaves. Thin film YIG 5 hrs have been used for the further FMR studied and confirmed the lowest spin-coated Gilbert damping constant α measured is $4.7 \pm 0.4 \times 10^{-3}$, and inhomogeneous contribution to the linewidth is 5.0 ± 0.3 mT. Sol-gel-based spin coating shows the potential to grow the polycrystalline YIG thin films with moderate magnetic energy dissipation.